Proposal number (User Support Office use only)

Date: October 12, 2018

Proposal for Nuclear Physics Experiment at RI Beam Factory

(RIBF NP-PAC-18, 2017)

Title of Experiment:	High Resolution In-Beam Gamma-Ray Spectrometer for the RIBF
Category:	[ ] NP experiment [ ] Detector R&D [X] Construction [ ] Update proposal (Experimental Program: NP____-____) [ ] Re-evaluation (Experimental Program: NP ____-____)
Experimental Devices:	[ ] GARIS [ ] RIPS [ ] CRIB [ ] KISS [X] BigRIPS [X] ZeroDegree [ ] SHARAQ [ ] OEDO [ ] RI Ring [ ] SAMURAI
Detectors:	[ ] DALI2 [ ] GRAPE

Spokesperson (Only one person, Multiple spokespersons not accepted):

Name	Pieter Doornenbal		
Institution	RIBF, RIKEN		
Title of position	Researcher		
Address	2-1 Hirosawa, Wako, Saitama 351-0198, Japan		
Tel.	+81 (0)48 462 1111	Fax	+81 (0)48 462 4464
Email	pieter@ribf.riken.jp		

Co-Spokesperson (if any):

Name	Kathrin Wimmer		
Institution	University of Tokyo		
Title of position	Lecturer		
Address	7-3-1 Hongo, Bunkyo-ku, TOKYO 113-0033 Japan		
Tel.	+81 (0)3-5841-4216	Fax	+81 (0)3-5841-7642
Email	wimmer@phys.s.u-tokyo.ac.jp		

Name			
Institution			
Title of position			
Address			
Tel.		Fax	
Email			

In-House Contact Person (if any):

Name			
Institution			
Title of position			
Address			
Tel.		Fax	
Email			

Beam Time Request Summary:
Please indicate requested beam times of $T_{User-Tuning}$ and $T_{User-DataRun}$ only. $T_{BigRIPS}$ and **Total** times will be given by RIKEN.

Total Beam Time	$T_{BigRIPS}$: Tuning time with BigRIPS for secondary beam settings	(User Support Office use only)	Days
	$T_{User-Tuning}$ Tuning time for users' own equipment and/or detectors using primary/secondary beams		Days
	$T_{User-DataRun}$ Beam-time for data runs		Days
Total		(User Support Office use only)	**Days**

Beam Summary
Primary Beam:

Particle		Energy	E/A (MeV)	Intensity	(pnA)

Secondary Beams:

RI Beams				Beam-On-Target Time for DATA RUN
Isotope	Energy $E/A(MeV)$	Rate of Isotope (/s)	Total Beam Rate @F3 (/s)	Days

Fill each row for each BigRIPS setting, with objective isotope, its energy, rate and total beam rate which cannot exceed 10^7/s in BigRIPS due to radiation regulation.

Keywords:

[ ]	New isotope search
[X]	Lifetime measurement
[ ]	Mass measurement
[ ]	Superheavy element
[ ]	β-γ spectroscopy
[X]	In-beam γ-ray spectroscopy [ ] 2_1^+ study
[X]	Nucleosynthesis [ ] r process [ ] rp process
[X]	Nuclear structure around [ ] ^{32}Mg [ ] ^{42}Si [ ] ^{78}Ni [ ] ^{100}Sn [ ] ^{132}Sn [ ] Others ( )
[X]	Nuclear reaction
[X]	Shell evolution
[ ]	Nuclear moment
[ ]	Spin-isospin excitation
[ ]	Nuclear force
[ ]	Nuclear equation of state
[ ]	Exotic atom
[X]	Isospin symmetry

Readiness:

Estimated date ready to run the experiment	2020
Date which should be excluded if any	—

Summary of Experiment:
It is proposed to construct a high-resolution, Ge based γ-ray spectrometer composed of the MINIBALL array as well as AGATA and GRETINA type cluster detectors named DAGATA, RCNP Quad, and LBNL P3. The envisioned in-flight resolution and efficiency are 0.15–1.5 % (σ) and 9.4%, respectively, for 1 MeV γ-rays emitted at 100 MeV/u. This setup will pave the way to detailed nuclear structure and reaction studies currently not feasible at the RIBF.

List of Collaborators (including spokespersons):

Name	Institution	Title or position	Email
N. Aoi	RCNP	Professor	aoi@rcnp.osaka-u.ac.jp
H. Baba	RIKEN	Team Leader	baba@ribf.riken.jp
F. Browne	RIKEN	Postdoc	frank@ribf.riken.jp
C. Campbell	LBNL	Researcher	cmcampbell@lbl.gov
M. Carpenter	ANL	Researcher	carpenter@phy.anl.gov
A. Corsi	CEA Saclay	Researcher	acorsi@cea.fr
M.L. Cortés	RIKEN	Postdoc	liliana@ribf.riken.jp
H. Crawford	LBNL	Researcher	hlcrawford@lbl.gov
M. Cromaz	LBNL	Researcher	mcromaz@lbl.gov
P. Doornenbal	RIKEN	Researcher	pieter@ribf.riken.jp
P. Fallon	LBNL	Researcher	pfallon@lbl.gov
A. Gillibert	CEA Saclay	Researcher	alain.gillibert@cea.fr
H. Hess	University of Cologne	Researcher	hess@ikp.uni-koeln.de
E. Ideguchi	RCNP	Assosciate Professor	ideguchi@rcnp.osaka-u.ac.jp
T. Isobe	RIKEN	Researcher	isobe@riken.jp
V. Lapoux	CEA Saclay	Researcher	valerie.lapoux@cea.fr
H. Liu	TU Darmstadt	Postdoc	hliu@ikp.tu-darmstadt.de
A. Macchiavelli	LBNL	Researcher	aomacchiavelli@lbl.gov
M. Niikura	The University of Tokyo	Assistant Professor	niikura@nucl.phys.s.u-tokyo.ac.jp
O. Möller	TU Darmstadt	Researcher	moeller@ikp.tu-darmstadt.de
S. Nishimura	RIKEN	Researcher	nishimu@ribf.riken.jp
A. Obertelli	TU Darmstadt	Professor	aobertelli@ikp.tu-darmstadt.de
V. Panin	CEA Saclay	Postdoc	valerii.panin@riken.jp
N. Pietralla	TU Darmstadt	Professor	pietralla@ikp.tu-darmstadt.de
P. Reiter	University of Cologne	Professor	preiter@ikp.uni-koeln.de
L. Riley	Ursinus College	Professor	lriley@ursinus.edu
H. Sakurai	The University of Tokyo/RIKEN	Chief Scientist	sakurai@ribf.riken.jp
M. Seidlitz	University of Cologne	Postdoc	seidlitz@ikp.uni-koeln.de
D. Suzuki	RIKEN	Researcher	daisuke.suzuki@ribf.riken.jp
S. Thiel	University of Cologne	Researcher	thiel@ikp.uni-koeln.de
V. Werner	TU Darmstadt	Researcher	vw@ikp.tu-darmstadt.de
N. Warr	University of Cologne	Researcher	warr@ikp.uni-koeln.de
K. Wimmer	The University of Tokyo	Lecturer	wimmer@phys.s.u-tokyo.ac.jp
Y. Yamamoto	RCNP	Researcher	yamamo@rcnp.osaka-u.ac.jp

Detailed Description of the proposed experiment

High Resolution In-Beam Gamma-Ray Spectrometer for the RIBF

Physics motivation

Since its first beam in 2006 the Radioactive Isotope Beam Factory (RIBF) of the RIKEN Nishina Center (RNC) provides highest intensity primary beams at 345 MeV/u. The great potential of the facility is best demonstrated by the search and discovery of more than 100 new isotopes [1–3] using a ^{238}U primary beam at the fragment separator BigRIPS [4]. In addition to ^{238}U, primary beams at the RIBF include ^{18}O, ^{48}Ca, ^{70}Zn, ^{124}Xe, and ^{78}Kr. In-beam γ-ray spectroscopy using secondary beams mostly employ the ZeroDegree spectrometer [4] for reaction product identification and the DALI2 NaI array [5] for γ-ray detection. Owing to the high secondary beam intensities as well as detection efficiency, experiments performed at the RIBF with the most exotic nuclei are feasible nowhere else in the world. Notable examples of the RIBF's capabilities include the first γ-ray spectroscopy of ^{54}Ca [6], ^{78}Ni [7], and ^{70}Kr [8]. Overall, in-beam γ-ray experiments currently account for $\approx$40 % of the physics publications from NP-PAC approved experiments at the RIBF with fast radioactive beams. A complete list of obtained results can be found in Ref. [9].
So far, spectroscopic experiments, carried out with the NaI(Tl) based spectrometer DALI2 [5], have been largely limited to even-even nuclei in the vicinity of shell closures. Using a germanium based γ-detector will significantly enhance the capabilities of the RIBF facility and open new possibilities for experiments. With this construction proposal, we combine the MINIBALL array [10], which contains 8 six-fold segmented triple clusters, an AGATA type triple [11] from the TU Darmstadt (referred to as DAGATA), a GRETINA type quad [12] from RCNP (referred to as RCNP Quad), and a GRETINA type triple from LBNL (referred to as LBNL P3) with the BigRIPS fragment separator and the ZeroDegree spectrometer [4]. This combination of the worlds highest secondary beam intensities with a Ge-based γ-ray spectrometer of 34 crystals in total will provide unique opportunities for nuclear structure as well as nuclear astrophysics studies.

1 Physics case

The RIBF provides currently worldwide uniquely high secondary beam intensities at intermediate energies ranging from 100 to 300 MeV/u. The proposed addition of the high resolution Ge-based γ-ray spectrometer will allow to access the most exotic nuclei and thus unprecedented science. Unique to the RIBF is the availability of a high intensity ^{238}U beam, giving access to the most neutron-rich nuclei around ^{78}Ni as well as heavier nuclei beyond ^{132}Sn which are of importance for the astrophysical r-process [13]. γ-ray spectroscopy experiments in this region of the nuclear chart can to date only be performed at the RIBF.

Shell evolution towards the drip-lines, new magic numbers

Neutron-rich nuclei below ^{78}Ni display many interesting features, halo systems have now

been suggested at $N \sim 20$ [14], while the classic shell gaps $N = 20, 28$ disappear for neutron-rich nuclei resulting in a large region of deformation [15, 16]. Tracking the evolution of the neutron $f_{7/2}$ and $p_{3/2}$ orbitals from $N = 20$ to 28 requires detailed spectroscopy of the even-odd nuclei. So far this has only been done for the Si isotopes [17] up to $N = 26$. Neutron knockout reactions with Ne or Mg isotopes would particularly benefit from the improved resolving power compared to DALI2.

In the Ca isotopic chain two new sub-shell closures have been established experimentally [6, 18, 19]. Theoretical calculations [20] show that three nucleon forces play an important role in the microscopic description of these nuclei. Spectroscopy of Ca isotopes at RIBF has recently been extended to $N = 36$ for 2_1^+ states and single-particle properties studied in the neutron and proton removal reactions from ^{54}Ca within the SEASTAR project [21]. Beyond Ca, the Ti isotopes show a staggering of collectivity which is not yet understood in either beyond mean field [22] as well as shell model [23] calculations. Lifetime measurements beyond the 2_1^+ states, the odd Ti isotopes, as well as spectroscopic factors obtained from knockout reaction will provide more stringent tests of the robustness of the closed-shell cores and the role of three-body forces for non-magic isotopes. Generally, due to the onset of collectivity and complexity of the level structures, odd-even nuclei beyond $Z = 20$ have been challenging with DALI2, as seen already for ^{55}Sc [24]. An abundance of new spectroscopic details may be revealed by utilizing high-resolution in-beam γ-ray spectroscopy.

Collectivity and breakdown of the harmonic oscillator shell closure at $N = 40$ has been established through measurements of collective properties, excitation energies, and level lifetimes (see for example Refs. [25–27] for most recent experimental data). A new island of inversion has been predicted with a center at ^{64}Cr [28]. Experimental data on spin and parity assignments as well as level occupations is sparse in the region of neutron-rich $N = 40$ nuclei. High-resolution spectroscopy of the even-odd nuclei ^{67,69}Fe, ^{63,65}Cr, and ^{57,59}Ti from one-neutron knockout reactions will fill this gap and reveal whether its inversion extends down towards ^{60}Ca.

Excited states in ^{78}Ni have recently been studied at the RIBF facility with a high intensity ^{238}U primary beam [7]. Quantification of the magnitude of the shell gap along $N = 50$ and $Z = 28$ as predicted in Ref. [29] requires precise measurements of odd nuclei through knockout reactions. Lifetime measurements of neutron-rich Zn, Ge, and Se nuclei with $N > 50$ to delineate the onset of collectivity beyond ^{78}Ni will be possible as well.

Structural changes around the doubly-magic ^{132}Sn are subject of great and persisting experimental as well as theoretical interest. Latest state-of-the-art Monte-Carlo Shell-Model calculations with an unprecedented large configuration space allowed for a detailed description of the structural evolution along the tin isotopic chain [30]. Predictions from this new interaction can be tested by knockout reactions from even tin isotopes as well by $B(E2)\uparrow$ measurements in ^{130,132,134}Sn.

North-east of ^{132}Sn, several interesting phenomena occur. E.g. the 6^+ seniority isomers along the Sn chain have been explored in the EURICA campaign [31]. The excitation energies of the 2_1^+ states in even-even isotopes are asymmetric with respect to $N = 82$ exhibiting lower values for $N < 82$. Filling the $2f_{7/2}$ neutron shell up to $N = 90$ some theories predict a similar behavior as for the Ca isotopic chain, resulting even in a new shell closure. However, in-beam data are hard to obtain for these neutron-rich isotopes. $(p, 2p)$ reactions in combination with high-resolution γ-ray spectroscopy open for the first time also access to odd isotopes. Moreover, the $(p, 2p)$ reactions will allow for the extraction of occupation numbers, shading new light on the underlying single-particle structures.

$N = Z$: the *rp*-process, mirror symmetry, and the quest for ^{100}Sn

Along the $N = Z$ line of the nuclear chart, a number of interesting physics cases can

be studied. Proton-rich nuclei along $N = Z$ constitute the path of the rapid proton-capture process (*rp*-process), that powers type I X-ray bursts. While direct measurements of (p,γ) reaction rates on these radioactive isotopes are not feasible in all cases, indirect measurements of excited states in the final nuclei as well as spectroscopic factors from (d,n) reactions can significantly reduce the uncertainties associated with the calculation of element abundances in the *rp*-process [32].

$N \sim Z$ nuclei also provide an interesting testing ground to investigate the breaking of charge symmetry and charge independence. Measurements of Coulomb energy and mirror energy differences have been limited so far to $A = 70$ and low spin values [8, 33]. Data for higher (medium) spin values and odd-even nuclei are required to clarify the role of isospin-non-conserving forces and neutron skin effects [34]. The high intensity ^{78}Kr and ^{124}Xe primary beams at RIBF combined with the high in-beam energy resolution of the Ge array allow for detailed spectroscopy of nuclei between $A = 50$ and 100. In addition to nuclear structure information, new data on waiting point nuclei of the *rp*-process predicted in this region can be obtained.

The region around ^{100}Sn has attracted a lot of interest. $B(E2)\uparrow$ values in light tin isotopes are larger than expected [35, 36], and the ordering of the neutron $\nu g_{7/2}$ and $\nu d_{5/2}$ orbitals above $N = 50$ seems to be inverted [37]. Spectroscopy of ^{101,103}Sn and ^{101,103}In through proton or neutron knockout and well as (p,p$'$) reactions will contribute to the understanding of unexpected high collectivity in the light even-even Sn nuclei.

Shape evolution and coexistence around $A \sim 100$ and in the rare earth region

Between $N = 50$ and $N = 82$, nuclei show an interesting interplay of single-particle and collective excitation modes. In the Sr and Zr isotopes, a sudden onset of collectivity at $N = 60$ is accompanied with shape coexistence at low excitation energies [38]. In the Kr isotopes, however, the associated drop in the $E(2_1^+)$ excitation energy is not observed [39, 40]. Additional information could come from lifetime measurements and off-yrast spectroscopy through secondary fragmentation reactions and spectroscopy of odd-even nuclei. High intensity radioactive beams with $Z \gtrsim 50$ are unique to the RIBF facility. Measurements of collective properties, excited state lifetimes, and proton inelastic scattering will shed new light on the evolution of collectivity and shape coexistence in this region. Measurements of single-particle properties will give hints on the underlying microscopic structure and new constraints for astrophysical *r*-process calculations.

Octupole collectivity in $A \sim 140$ and 90 nuclei

In regions where neutrons and protons occupy orbitals at the Fermi surface with $\Delta j = \ell = 3$ strong octupole correlations can break the reflection symmetry of nuclei, resulting in octupole deformed shapes. Octupole collectivity is expected below the Ra-Th region for neutron-rich nuclei in the region around ^{90}Se and ^{144}Ba [41]. In the first case, first spectroscopy of ^{90}Se has only been performed recently [42], and measurements beyond the spectroscopy of states are necessary to asses the possibility of octupole deformation, for example by lifetime measurements.

2 High-resolution in-beam γ-ray spectroscopy at the RIBF

It is proposed to couple a high-resolution Ge array with the BigRIPS fragment separator and the ZeroDegree spectrometer at the RIBF. Experimental details are briefly described in the following section, highlighting the unrivaled possibilities for in-beam γ-ray spectroscopy experiments offered at the RIBF.

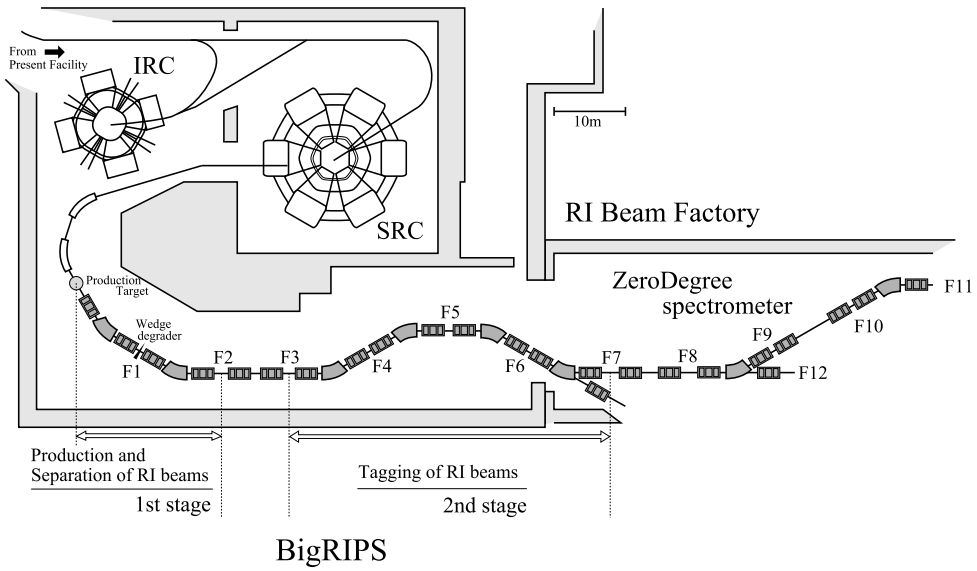

Figure 1: Overview of the RIBF facility. Not shown are the initial acceleration stages. The BigRIPS fragment separator is used to purify and identify the radioactive ion beams (production target – F7). The array will be placed the focal point F8. Reaction products are uniquely identified using the ZeroDegree spectrometer (F8 – F11).

2.1 BigRIPS and ZeroDegree spectrometer

A layout of the RIBF facility is presented in Fig. 1. Primary beams impinge on the production target (F0); their fragmentation or fission products are subsequently separated in the two-stage separator BigRIPS. Event-by-event identification is facilitated by $B\rho$, ΔE, and time-of-flight measurements between the focal points F3 and F7. Positions and angles of beam particles are measured using parallel plate avalanche counters (PPAC), the time-of-flight is measured with plastic scintillators at F3 and F7. At F7, an ionization chamber allows for unique Z identification through an energy loss measurement. Maximum rates are several tens of kHz. The total momentum acceptance amounts to ± 3 % with a momentum resolution of 3420 ($p/\delta p$). A relative A/Q resolution of 0.034 % has been achieved [43], allowing for the separation of fully stripped from hydrogen-like charge states. Production cross sections of radioactive ions have been measured for a wide range of nuclei [2, 3, 44] providing validation of the theoretical fragmentation and fission cross sections employed in LISE++ simulations. Secondary beam intensities for experiments can therefore be predicted reliably allowing for an easy planning of experiments at the RIBF.

In-beam γ-ray spectroscopy experiments are performed at F8 with thick solid secondary reaction targets (Be, C, Au, Pb etc.) in the order of 1 g/cm^2 depending on the case of interest. The size of the beam spot on the target amounts typically to $\sigma = 5$ mm. Tracking of the beam onto the target is facilitated by a set of two PPACs in front of the target (position resolution $\sigma = 0.7$ mm), the scattering angle can be reconstructed using a third PPAC behind the target (before STQ17 in Fig. 1) with an accuracy of typically 5 mrad [36]. For the high-resolution array, we envision to use either solid targets, the liquid hydrogen target MINOS [45], or plunger for lifetime measurements. For experiments with solid targets, the present setup at F8 with three PPACs and a beam pipe of 150 mm diameter can be maintained.

The ZeroDegree spectrometer will be used for identification of reaction products after the secondary target located at F8 (see Fig. 1). Particle identification will be obtained in an analogous way to the BigRIPS separator by using $B\rho$, ΔE, and time-of-flight measurements between F8 and F11. Typical beam energies after the target will amount to $100 - 200$ MeV/u. Therefore, for high Z nuclei not all reaction products will be in the fully stripped charge state. With the

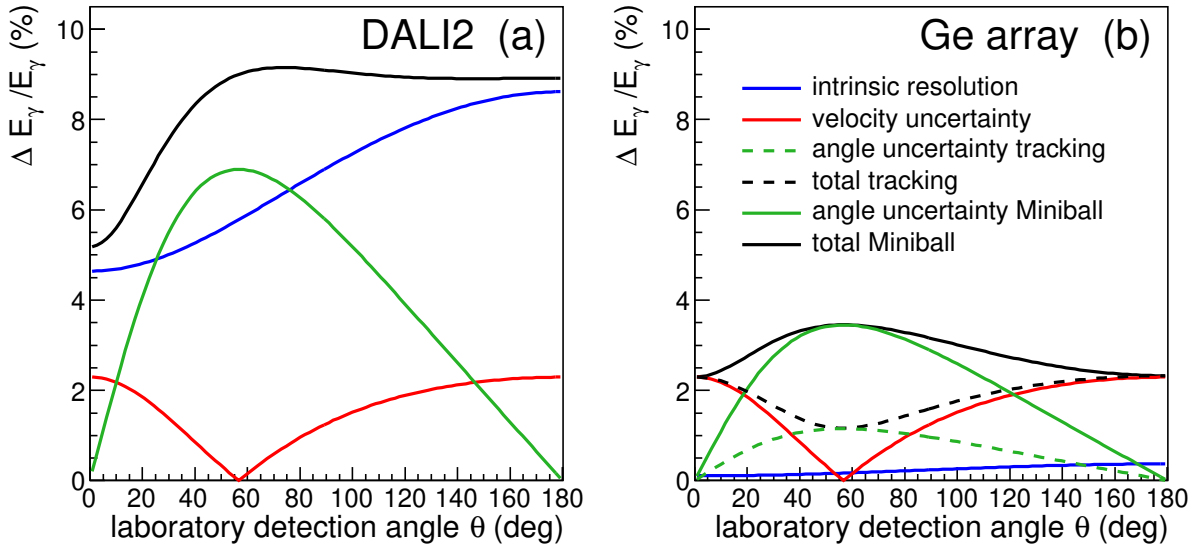

Figure 2: Energy resolution of high-resolution array (b) in comparison with DALI2 (a). The total in-beam energy resolution (black) depends on the intrinsic energy resolution (blue), the position resolution for the Doppler correction (green) as well as the velocity uncertainty due to the energy loss in the target (red). Uncertainties are calculated for a 200 MeV/u beam impinging on a 4 mm Be secondary target ($\langle\beta\rangle = 0.55$, $\Delta\beta = 0.016$) emitting a 1 MeV γ ray. Great improvements in the intrinsic energy as well a position resolution of the high-resolution array compared to DALI2 allow for spectroscopy with about 1–3 % final energy resolution for in-beam experiments. This assumes Doppler correction on the segment level for MINIBALL, and a position resolution of 5 mm (FWHM) for DAGATA, RCNP Quad, and LBNL P3 detectors. Detectors are placed at a distance of 200 mm.

high resolution for the mass to charge ratio A/Q it is possible to discriminate different charge states up to $Z \approx 55$, $A \approx 150$. Additionally, a total kinetic energy detector can be placed at the end of the beam-line after the last ionization chamber at F11. With a momentum resolution of $p/\Delta p = 1240$ the large acceptance mode offers sufficient accuracy for parallel momentum distributions to deduce angular momentum L assignments.

2.2 High resolution Ge spectrometer

In-beam γ-ray spectroscopy at the RIBF has so far been mostly restricted to the spectroscopy of even-even nuclei. Spectroscopy of odd nuclei is challenging due to the limited energy resolution, except for certain cases close to magic numbers [24, 46]. The in-beam energy resolution depends critically on the intrinsic energy as well as position resolution, as shown in Fig. 2 (a).
Here, we propose to combine the existing MINIBALL array, DAGATA, the RCNP Quad, and the LBNL P3 to a common array of 34 crystals. The latter three are 36-fold segmented, position sensitive γ-ray tracking detectors, while MINIBALL consists of eight six-fold segmented triple clusters. It is noted that the collaboration has experience in running and maintaining such position sensitive detectors.
Obtainable energy resolutions following Doppler correction depend largely on distance and angle of the placed detectors. Assuming detector distances of 200 mm, the resolution is improved by a factor three for MINIBALL detectors and about a factor five to ten for γ-ray tracking detectors compared to DALI2, but these numbers also depends on the energy loss inside the reaction target. Fig. 2 shows the parameters of a typical in-beam γ-ray experiment at the RIBF. For larger distances between detectors and target, better resolutions can be obtained.
The nominal efficiency of MINIBALL amounts to 7.8 % at 1.3 MeV [10] using add-back. For ex-

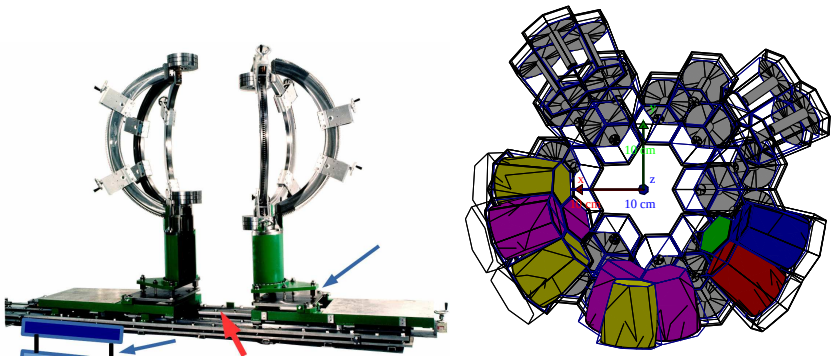

Figure 3: (Left) Support structure for the array. The system will be placed on rails (red arrow) and can be height adjusted to the BigRIPS/ZeroDegree beam height of 1700 mm. Detectors can be placed at desired angles. (Right) Possible configuration of the array as seen from upstream in GEANT4 simulations. MINIBALL crystals are shown in gray, the RCNP Quad and LBNL P3 in yellow and purple, and DAGATA in red, green, and blue.

periments at RIBF, the distance to the target is larger than for the typical experiments performed at REX-ISOLDE. Thus a reduced efficiency is expected. For experiments with fast beams performed at GSI, the array was placed at angles of 51 and 85° at about 220 mm distance, resulting in a resolution of 3 % and an efficiency of 3 % for a 1.3 MeV γ-ray emitted at 100 MeV/u [47]. Due to their position resolution of 5 mm (FWHM), the tracking detectors can be positioned much closer to the reaction target. Assuming a distance of 130 mm, which sets the resolution to about 1–3 %, the total efficiency of the entire array amounts around 9 %. Due to the beam pipe diameter of 150 mm, such close distances are not available for all angles.

2.3 Support structure

The MINIBALL support structure, shown in Fig. 3 fits into the F8 area, which offers 2 m of space along the beam axis between the F8 chamber and STQ17. The beam height at F8 is 1.7 m. All 11 detectors can be attached to the three rings. Angles and distances can be varied according to the specific requirements of the experiment.

2.4 Simulations of resolution and efficiency

Initial simulations based on the GEANT4 framework [48] have been carried out. Parameters and obtained results are summarized in Tab. 2. The simulations comprised MINIBALL, DAGATA,

Detector	Crystals	Angle	Distance / mm	Resolution / %	Efficiency /%
MINIBALL	18	30	200	1.03	4.1
MINIBALL	6	65	200	1.52	1.1
RCNP Quad, LBNL P3	7	65	130	0.15	3.1
DAGATA	3	65	130	0.16	1.1
Total	34				9.4

Table 2: Simulated energy resolution (σ) and efficiency for a 1 MeV γ-ray emitted at 100 MeV/u. The RCNP Quad, the LBNL P3, and DAGATA can be placed much closer to the target due to their enhance position resolution. Presented values include intra cluster add-back and Doppler correction based on segment level for MINIBALL and (link-algorithm based) interaction point clustering and tracking to find the first interaction point for the tracking detectors.

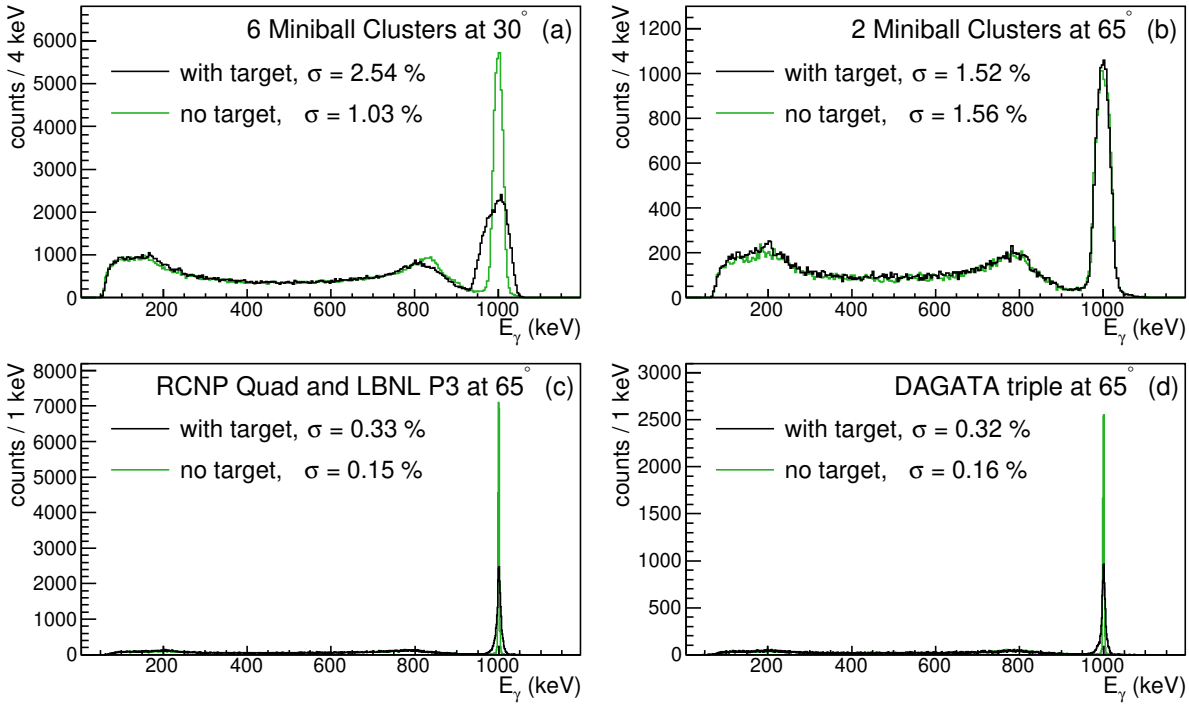

Figure 4: Doppler Corrected energy spectra for a 1 MeV γ-ray emitted at 100 MeV/u without target and with a 3 mm Be target. The latter uses ^{79}Cu secondary beams. See text for details.

the RCNP Quad, and the LBNL P3. Simulations were carried out for a 1 MeV γ-ray emitted at 100 MeV/u. As seen in Fig 2, MINIBALL crystals are best placed at forward angles, while angles around 60° are ideal for the tracking detectors. For the angles given in Tab. 2, this resulted in a resolution between 0.15–1.5 % (σ) and an efficiency of 9.4 %. A position reconstruction resolution of 5 mm (FWHM), which has been verified in various experiments, was taken for the tracking detectors. Obtained Doppler corrected energy spectra are displayed in Fig. 4, while the configuration is shown in Fig. 3.

Usage of thick solid target may impede the obtainable energy resolution significantly, as illustrated in Fig. 4 for a ^{79}Cu beam impinging on a 3 mm-thick Be target. Such cases will greatly benefit from liquid hydrogen targets in combination with the time projection chamber surrounding MINOS. In 2020, a new compact Si tracker named Strasse should be available at the RIBF [49]. It could be considered for experiments requiring the luminosity provided by a thick H2 target with a significant gain in energy resolution.

It is noted that the employed configuration may vary from the one presented here, depending on the experimental program. However, MINIBALL detectors are shorter than the tracking detectors. Due to the limited space at F8 (1255 mm between the F8 standard focal point and STQ17), MINIBALL detectors fit at forward angles.

3 Required equipment

The RIBF has ample experience with hosting Ge detector arrays, for example hosting EURICA from 2012–2016 [50, 51]. Though, some infrastructure from the EURICA campaign exists and can be used for the array, vital instrumentation is missing. Particularly, high voltage supply, monitoring, UPS, and a reliable liquid nitrogen system are required as infrastructure.

A harmonized data acquisition system is indispensable for a smooth readout of the individual systems. This electronic readout will be based on the readout implemented for GRETINA, requiring a total of 568 readout channels due to the six-fold segmentation of a MINIBALL

Budget required for Array			57,400 (x 1k ¥)
Item	Cost	Item	Cost
Travel	2,000	Maintenance Ge	2,000
Pumping system	1,600	HV Power	5,000
UPS	2,000	Liq. N2 system	3,000
Liq. N2 Dewar	3,500	Cooling pipes	400
Shipping	2,000	Rail system	4,000
Digitizer	10,000	Trigger modules	2,500
VME crates	1,400	IOC	4,000
Computer Cluster	10,000		

Table 3: Estimated costs necessary to implement the described high resolution array at the RIBF.

crystal and 36-fold segmentation of DAGATA, RCNP Quad, and LBNL P3 (40 per tracking type crystal, 7 per MINIBALL crystal including core signals). The total readout costs (digitizer, trigger module, VME crate, computing power, etc.) are estimated to be 120,000¥ per channel. Some of the electronics are already available. However, readout electronics for DAGATA and MINIBALL array are necessary, but may be partially borrowed from the CAGRA project [52]. It is estimated that electronic equipment for 200 readout channels will be needed to be purchased. Other incurring costs include the shipment of the MINIBALL detectors and support structure from the University of Cologne, and setting up a rail system at F8. Furthermore, travel support is necessary to setup the detectors at the RIBF. A summary of expected costs is provided in Tab. 3.

4 Project time-line

In parallel to this construction proposal, the collaboration is submitting a Letter of Intent to host MINIBALL at the RIBF in 2020. The next MINIBALL Steering Committee meeting will be held by the end of 2018.
It is foreseen to hold a dedicated workshop in spring 2019, either at RIBF or in Europe, to discuss the physics proposals and details of the setup. Applications for beam time with this proposed array in future NP-PACs will be open to all RIBF users. The MINIBALL array will be available for experiments at the RIBF in the calendar year 2020, while other detectors of the array may be further available.

References

[1] T. Ohnishi et al. *J. Phys. Soc. Jpn.*, 79:073201, 2010.

[2] Y. Shimizu et al. *J. Phys. Soc. Jpn.*, 87:014203, 2018.

[3] N. Fukuda et al. *J. Phys. Soc. Jpn.*, 87:014202, 2018.

[4] T. Kubo et al. *Prog. Theor. Exp. Phys.*, 2012:03C003, 2012.

[5] S. Takeuchi et al. *Nucl. Instrum. and Methods Phys. Res. A*, 763:596, 2014.

[6] D. Steppenbeck et al. *Nature*, 502:207, 2013.

[7] R. Taniuchi. *In-beam gamma-ray spectroscopy of* ^{78}*Ni*. PhD thesis, The University of Tokyo, 2018.

[8] K. Wimmer et al. *Physics Letters B*, 785:441 – 446, 2018.

[9] SUNFLOWER publications. `http://www.nishina.riken.jp/collaboration/SUNFLOWER/publication/bigrips.html`, 2018.

[10] N. Warr et al. *Eur. Phys. J. A*, 49:40, 2013.

[11] S. Akkoyun et al. *Nucl. Instr. Meth. A*, 668:26, 2012.

[12] S. Paschalis et al. *Nucl. Instrum. Methods Phys. Res. A*, 709:44, 2013.

[13] G. Lorusso et al. *Phys. Rev. Lett.*, 114:192501, 2015.

[14] T. Nakamura et al. *Phys. Rev. Lett.*, 112:142501, 2014.

[15] P. Doornenbal et al. *Phys. Rev. Lett.*, 111:212502, 2013.

[16] E. Caurier, F. Nowacki, and A. Poves. *Phys. Rev. C*, 90:014302, 2014.

[17] S. R. Stroberg et al. *Phys. Rev. C*, 91:041302, 2015.

[18] F. Wienholtz et al. *Nature*, 498:346, 2013.

[19] S. Michimasa et al. *Phys. Rev. Lett.*, 121:022506, 2018.

[20] J. D. Holt et al. *Phys. Rev. C*, 90:024312, 2014.

[21] SEASTAR project. `http://www.nishina.riken.jp/collaboration/SUNFLOWER/experiment/seastar/index.html`, 2018.

[22] Tomás R. Rodríguez and J. Luis Egido. *Phys. Rev. Lett.*, 99:062501, 2007.

[23] L. Coraggio, A. Covello, A. Gargano, and N. Itaco. *Phys. Rev. C*, 89:024319, 2014.

[24] D. Steppenbeck et al. *Phys. Rev. C*, 96:064310, 2017.

[25] H. L. Crawford et al. *Phys. Rev. Lett.*, 110:242701, 2013.

[26] A. Gade et al. *Phys. Rev. Lett.*, 112:112503, 2014.

[27] C. Santamaria et al. *Phys. Rev. Lett.*, 115:192501, 2015.

[28] S. M. Lenzi et al. *Phys. Rev. C*, 82:054301, 2010.

[29] Y. Tsunoda et al. *Phys. Rev. C*, 89:031301, 2014.

[30] T. Togashi et al. *Phys. Rev. Lett.*, 121:062501, 2018.

[31] G. Simpson et al. *Phys. Rev. Lett.*, 113:132592, 2014.

[32] C. Langer et al. *Phys. Rev. Lett.*, 113:032502, 2014.

[33] A. Obertelli et al. *Physics Letters B*, 701:417 – 421, 2011.

[34] A. Boso et al. *Phys. Rev. Lett.*, 121:032502, 2018.

[35] V. M. Bader et al. *Phys. Rev. C*, 88:051301, 2013.

[36] P. Doornenbal et al. *Phys. Rev. C*, 90:061302, 2014.

[37] I. G. Darby et al. *Phys. Rev. Lett.*, 105:162502, 2010.

[38] P. Federman and S. Pittel. *Phys. Rev. C*, 20:820, 1979.

[39] M. Albers et al. *Phys. Rev. Lett.*, 108:062701, 2012.

[40] F. Flavigny et al. *Phys. Rev. Lett.*, 118:242501, 2017.

[41] B. Bucher et al. *Phys. Rev. Lett.*, 116:112503, 2016.

[42] S. Chen et al. *Phys. Rev. C*, 95:041302, 2017.

[43] N. Fukuda et al. *Nucl. Instrum. Methods Phys. Res. B*, 317:323, 2013.

[44] H. Suzuki et al. *Nucl. Instrum. Methods Phys. Res. B*, 317:756, 2013.

[45] A. Obertelli et al. *Eur. Phys. J. A*, 50:8, 2014.

[46] L. Olivier et al. *Phys. Rev. Lett.*, 119:192501, 2017.

[47] P. Doornenbal. *In-beam γ-ray spectroscopy of two-step fragmentation reactions at relativistic energies - The case of ^{36}Ca.* PhD thesis, Universität zu Köln, 2007.

[48] S. Agostinelli et al. *Nucl. Instr. Meth. A*, 506:250, 2003.

[49] Construction proposal: Large-acceptance missing mass setup at samurai. Submitted to the 19$^{\text{th}}$ RIBF NP-PAC, 2018.

[50] S. Nishimura. *Prog. Theor. Exp. Phys.*, 2012:03C003, 2012.

[51] P.A. Söderström et al. *Nucl. Instr. Meth. B*, 317:649, 2013.

[52] CAGRA project. `http://www.rcnp.osaka-u.ac.jp/Divisions/np1-a/CAGRA/index.html`, 2018.